*Int. J. Heat Mass Transfer.* Vol. 27, No. 6, pp. 911–920, 1984
Printed in Great Britain

0017–9310/84 $3.00 + 0.00
Pergamon Press Ltd.

# A SIMILARITY RELATION FOR ENERGY SEPARATION IN A VORTEX TUBE

K. STEPHAN,† S. LIN,‡ M. DURST,† F. HUANG§ and D. SEHER†

† Institut für Technische Thermodynamik und Thermische Verfahrenstechnik, Universität Stuttgart, Federal Republic of Germany; ‡ Department of Mechanical Engineering, Concordia University Montreal, Canada; § Peking Institute of Aeronautics and Astronautics, Department of Aircraft Engineering, Peking, China

(*Received* 21 *April* 1983)

**Abstract**—A general mathematical formulation of the energy separation process taking place in a vortex tube is presented. Based on the governing equations a similarity relation of the variation of the cold gas exit temperature with the cold gas mass ratio for geometrically similar vortex tubes is established and compared with experimental data. The experiments conducted with air, helium and oxygen as working media confirm the theoretical considerations and correspond very well with the similarity relation.

## NOMENCLATURE

| | |
|---|---|
| $c_p$ | specific heat at constant pressure |
| $D$ | inner diameter of vortex tube |
| $d, D$ | diameter and dimensionless diameter, respectively |
| $E$ | dimensionless parameter |
| $k$ | thermal conductivity |
| $L, L^*$ | length and dimensionless length of vortex tube, respectively |
| $\dot{m}$ | mass flow rate |
| $p, p^*$ | pressure and dimensionless pressure, respectively |
| $p_\infty, p_\infty^*$ | ambient pressure and dimensionless ambient pressure, respectively |
| $Pr$ | Prandtl number |
| $r, \theta, z$ | cylindrical coordinates |
| $R$ | dimensionless radial coordinate |
| $R, R^*$ | gas constant and dimensionless gas constant, respectively |
| $Re$ | Reynolds number |
| $T, \theta$ | temperature and dimensionless temperature, respectively |
| $\Delta T$ | temperature difference |
| $v, V$ | velocity vector and dimensionless velocity vector, respectively |
| $v_r, v_\theta, v_z$ | velocity components in the $r$-, $\theta$-, and $z$-directions, respectively |
| $V_R, V_\theta, V_Z$ | dimensionless velocity components in the $R$-, $\theta$-, and $Z$-directions, respectively |
| $w_0$ | inlet velocity |
| $x$ | warm gas mass ratio |
| $y$ | cold gas mass ratio |
| $z, Z$ | axial coordinate and dimensionless axial coordinate, respectively. |

Greek symbols

| | |
|---|---|
| $\beta, \beta^*$ | coefficient of thermal expansion and dimensionless coefficient of thermal expansion, respectively |
| $\delta, \Delta$ | width and dimensionless width of the inlet part of the vortex tube, respectively |
| $\mu$ | dynamic viscosity |
| $\rho, \rho^*$ | density and dimensionless density, respectively |
| $\tau, \tau^*$ | viscous stress tensor and dimensionless viscous stress tensor, respectively. |

Subscripts

| | |
|---|---|
| c | cold gas |
| h | hot gas |
| w | wall |
| 0 | inlet. |

## 1. INTRODUCTION

THE VORTEX tube is a simple device operating as a refrigerating machine without any moving components, e.g. rotating shafts or cylinders. It consists mainly of a simple tube. A compressed gas flows tangentially with a high velocity into the vortex tube. Right next to the entrance nozzle a cold gas stream leaves the tube through a central orifice, while at the far end of the tube a hot gas stream near the wall is exhausted.

The phenomenon of energy separation in a vortex tube was first reported by Ranque [1]. Important experimental investigations were conducted by Hilsch [2], Elser and Hoch [3], Martynovskii and Alekseev [4], Takahama [5], Hartnett and Eckert [6] and Bobrovnikov *et al.* [7]. Theoretical and analytical descriptions of the energy separation and the temperature and velocity profiles in a vortex tube were given by Fulton [8], Schultz-Grunow [9], Erdélyi [10], Alekseev and Azaroff [11] and Deissler and Perlmutter [12]. An industrial application of the natural gas was reported by Raiskii and Sedykh [13]. Successful attempts in the application of gas separation by a vortex tube were done by Linderstrøm-Lang [14], Marshall [15] and Igonin *et al.* [16].

Recently an experimental investigation of the energy separation process in the vortex tube with air as a working medium was conducted [17]. Experimental results indicate that the Görtler vortex produced by the

tangential velocity on the inside wall of the vortex tube is a main driving force for the energy separation in the vortex tube. By making use of the dimensional analysis a similarity relation of the cold gas exit temperature with the cold gas mass ratio was also established and confirmed by the experimental data.

In this paper a general mathematical formulation of the energy separation process in a vortex tube is presented. From the system of equations formulated, a similarity relation for prediction of the cold gas temperature is established, which confirms the similarity relation obtained by the dimensional analysis described in ref. [17]. Further experimental results with oxygen and helium as working media in the vortex tube used in ref. [17] are also reported and confirm the similarity relation.

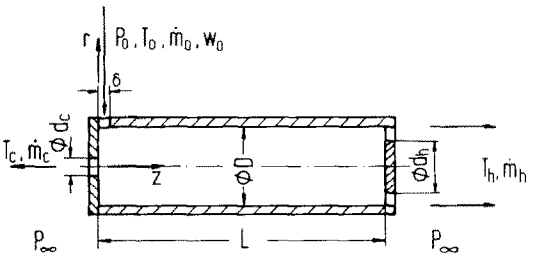


FIG. 1. Schematic diagram of the geometrical configuration of the vortex tube.

## 2. MATHEMATICAL FORMULATION

We consider a steady-state, axisymmetrical compressible flow in a vortex tube with negligible body force and without an energy source as shown in Fig. 1. The vortex tube is well insulated from its surroundings. The gas flowing through the vortex tube is considered as an ideal gas.

The system of equations describing the energy separation process in the vortex tube can be expressed as follows:

(1) Continuity equation

$$\frac{1}{r}\frac{\partial}{\partial r}(\rho r v_r)+\frac{\partial}{\partial z}(\rho v_z)=0. \tag{1}$$

(2) Viscous stress equation of motion [18]:

in $r$-direction

$$\rho\left(v_r\frac{\partial v_r}{\partial r}-\frac{v_\theta^2}{r}+v_z\frac{\partial v_r}{\partial z}\right) = -\frac{\partial p}{\partial r}+\left[\frac{1}{r}\frac{\partial}{\partial r}(r\tau_{rr})-\frac{\tau_{\theta\theta}}{r}+\frac{\partial\tau_{zr}}{\partial z}\right]; \tag{2}$$

in $\theta$-direction

$$\rho\left(v_r\frac{\partial v_\theta}{\partial r}+\frac{v_r v_\theta}{r}+v_z\frac{\partial v_\theta}{\partial z}\right)=\left[\frac{1}{r^2}\frac{\partial}{\partial r}(r^2\tau_{r\theta})+\frac{\partial\tau_{z\theta}}{\partial z}\right]; \tag{3}$$

in $z$-direction

$$\rho\left(v_r\frac{\partial v_z}{\partial r}+v_z\frac{\partial v_z}{\partial z}\right)=-\frac{\partial p}{\partial z}+\left[\frac{1}{r}\frac{\partial}{\partial r}(r\tau_{rz})+\frac{\partial\tau_{zz}}{\partial z}\right]. \tag{4}$$

Here $\tau$ is the viscous stress tensor which can be described by [19]

$$\tau=\mu\begin{bmatrix} 2\left(\frac{\partial v_r}{\partial r}-\frac{1}{3}\operatorname{div} v\right) & \left(\frac{\partial v_\theta}{\partial r}-\frac{v_\theta}{r}\right) & \left(\frac{\partial v_r}{\partial z}+\frac{\partial v_z}{\partial r}\right) \\ \left(\frac{\partial v_\theta}{\partial r}-\frac{v_\theta}{r}\right) & 2\left(\frac{v_r}{r}-\frac{1}{3}\operatorname{div} v\right) & \frac{\partial v_\theta}{\partial z} \\ \left(\frac{\partial v_r}{\partial z}+\frac{\partial v_z}{\partial r}\right) & \frac{\partial v_\theta}{\partial z} & 2\left(\frac{\partial v_z}{\partial z}-\frac{1}{3}\operatorname{div} v\right) \end{bmatrix}. \tag{5}$$

(3) Thermal energy equation [18]

$$\rho c_p\left(v_r\frac{\partial T}{\partial r}+v_z\frac{\partial T}{\partial z}\right)=\frac{1}{r}\frac{\partial}{\partial r}\left(rk\frac{\partial T}{\partial r}\right)+\frac{\partial}{\partial z}\left(k\frac{\partial T}{\partial z}\right) + T\beta\left(v_r\frac{\partial p}{\partial r}+v_z\frac{\partial p}{\partial z}\right)+\nabla v:\tau, \tag{6a}$$

where $\nabla v:\tau$ is the viscous dissipation function which can be expressed for Newtonian fluids by

$$\nabla v:\tau=2\mu\left[\left(\frac{\partial v_r}{\partial r}\right)^2+\left(\frac{v_r}{r}\right)^2+\left(\frac{\partial v_z}{\partial z}\right)^2\right] +\mu\left[r\frac{\partial}{\partial r}\left(\frac{v_\theta}{r}\right)\right]^2+\mu\left[\frac{\partial v_\theta}{\partial z}\right]^2+\mu\left[\frac{\partial v_r}{\partial z}+\frac{\partial v_z}{\partial r}\right]^2. \tag{6b}$$

(4) *Equation of state*

$$\frac{p}{\rho}=RT. \tag{7}$$

There are six unknowns $v_r$, $v_\theta$, $v_z$, $p$, $T$, and $\rho$, with six equations, equations (1)–(4), (6a) and (7).

The boundary conditions required to solve the problem can be described as (see Fig. 1)

$$\begin{aligned} v_r=0 \quad \text{for} \quad & z=0, && 0<r<\frac{D}{2}, \\ & z=L, && 0<r<\frac{D}{2}, \\ & 0<z<L, && r=0, \\ & 0<z<L, && r=\frac{D}{2}, \end{aligned} \tag{8}$$

$$v_z = 0 \quad \text{for} \quad z = 0, \quad \frac{d_c}{2} < r < \frac{D}{2}, \tag{9}$$

$$z = L, \quad 0 < r < \frac{d_h}{2},$$

$$0 < z < L, \quad r = \frac{D}{2},$$

$$\frac{\partial v_z}{\partial r} = 0 \quad \text{for} \quad 0 < z < L, \quad r = 0, \tag{10}$$

$$v_\theta = 0 \quad \text{for} \quad z = 0, \quad \frac{d_c}{2} < r < \frac{D}{2}, \tag{11}$$

$$z = L, \quad 0 < r < \frac{d_h}{2},$$

$$0 < z < L, \quad r = 0,$$

$$\delta < z < L, \quad r = \frac{D}{2},$$

$$v_\theta = w_0 \quad \text{for} \quad 0 < z < \delta, \quad r = \frac{D}{2}, \tag{12}$$

$$p = p_0 \quad \text{for} \quad 0 < z < \delta, \quad r = \frac{D}{2}, \tag{13}$$

$$p = p_\infty \quad \text{for} \quad z = 0, \quad 0 < r < \frac{d_c}{2}, \tag{14}$$

$$z = L, \quad \frac{d_h}{2} < r < \frac{D}{2},$$

$$T = T_0 \quad \text{for} \quad 0 < z < \delta, \quad r = \frac{D}{2}, \tag{15}$$

$$\frac{\partial T}{\partial r} = 0 \quad \text{for} \quad \delta < z < L, \quad r = \frac{D}{2}, \tag{16}$$

$$0 < z < L, \quad r = 0,$$

$$\frac{\partial T}{\partial z} = 0 \quad \text{for} \quad z = 0, \quad \frac{d_c}{2} < r < \frac{D}{2}, \tag{17}$$

$$z = L, \quad 0 < r < \frac{d_h}{2}.$$

At the outlets the total outlet mass flow rate must be equal to the inlet mass flow rate and the total outlet energy must be equal to the inlet energy

$$\dot{m}_c + \dot{m}_h = \dot{m}_0, \tag{18}$$

where

$$\dot{m}_c = 2\pi \int_0^{d_c/2} \rho |v_z| r \, dr, \tag{19}$$

and

$$\dot{m}_h = 2\pi \int_{d_h/2}^{D/2} \rho v_z r \, dr, \tag{20}$$

and

$$\dot{m}_c \left( c_{pc} T_c + \frac{v_{zc}^2 + v_{\theta c}^2}{2} \right) + \dot{m}_h \left( c_{ph} T_h + \frac{v_{zh}^2 + v_{\theta h}^2}{2} \right) = \dot{m}_0 \left( c_{p0} T_0 + \frac{w_0^2}{2} \right), \tag{21}$$

where $T_c$, $v_{zc}$ and $v_{\theta c}$ are the mean values of the temperature, axial velocity component and tangential velocity component at the outlet of the cold gas, respectively, and $T_h$, $v_{zh}$ and $v_{\theta h}$ are the mean values of the temperature, axial velocity component and tangential velocity component at the outlet of the hot gas, respectively. These values are unknown. They have to be determined as a part of the solution of the problem.

It can be seen that the above system of equations is nonlinear, and the boundary conditions are complicated and some of them are unknown and are dependent on the solution of the problem. Therefore a mathematical treatment of such a problem is quite difficult if not impossible at present.

For energy separation in a vortex tube, the temperature of the cold exit gas is the most important variable to be determined. For the purpose of obtaining a similarity relation for predicting the cold gas temperature, the system of equations, equations (1)–(21), will first be transformed into a dimensionless form.

## 3. SIMILARITY RELATION FOR PREDICTION OF THE COLD GAS TEMPERATURE

For the purpose of transforming the system of equations into a dimensionless form, we consider the variation of the material properties, $\mu$, $k$, $c_p$, and $\beta$ in the operating range to be negligibly small and introduce the following dimensionless variables and parameters:

$$\left.\begin{aligned}
R &= \frac{r}{D}, & P^* &= \frac{p}{\rho_0 w_0^2},\\
Z &= \frac{z}{D}, & P_0^* &= \frac{p_0}{\rho_0 w_0^2},\\
D_c &= \frac{d_c}{D}, & P_\infty^* &= \frac{p_\infty}{\rho_0 w_0^2},\\
D_h &= \frac{d_h}{D}, & \theta &= \frac{T}{T_0},\\
\Delta &= \frac{\delta}{D}, & \theta_c &= \frac{T_c}{T_0},\\
L^* &= \frac{L}{D}, & \theta_h &= \frac{T_h}{T_0},\\
\mathrm{div}^* &= D\,\mathrm{div}, & Re &= \frac{\rho_0 w_0 D}{\mu},\\
\nabla^* &= D\nabla, & Pr &= \frac{c_p \mu}{k},\\
V_R &= \frac{v_r}{w_0}, & E &= \frac{w_0^2}{c_p T_0},\\
V_\theta &= \frac{v_\theta}{w_0}, & R^* &= \frac{R T_0}{w_0^2},\\
V_z &= \frac{v_z}{w_0}, & \beta^* &= \frac{\beta w_0^2}{c_p},\\
V &= \frac{v}{w_0}, & y &= \frac{\dot{m}_c}{\dot{m}_0},\\
\rho^* &= \frac{\rho}{\rho_0}, & x &= \frac{\dot{m}_h}{\dot{m}_0} = 1 - y.
\end{aligned}\right\} \tag{22}$$

Making use of these dimensionless variables and parameters, the system of equations, equations (1)–(21) transforms into

$$\frac{1}{R}\frac{\partial}{\partial R}(\rho^* R V_r)+\frac{\partial}{\partial Z}(\rho^* V_z)=0, \tag{23}$$

$$\rho^*\left(V_R\frac{\partial V_R}{\partial R}-\frac{V_\theta^2}{R}+V_Z\frac{\partial V_R}{\partial Z}\right) = -\frac{\partial P^*}{\partial R}-\left[\frac{1}{R}\frac{\partial}{\partial R}(R\tau^*_{RR})-\frac{\tau^*_{\theta\theta}}{R}+\frac{\partial\tau^*_{ZR}}{\partial Z}\right], \tag{24}$$

$$\rho^*\left(V_R\frac{\partial V_\theta}{\partial R}+\frac{V_R V_\theta}{R}+V_Z\frac{\partial V_\theta}{\partial Z}\right) = \left[\frac{1}{R^2}\frac{\partial}{\partial R}(R^2\tau^*_{R\theta})+\frac{\partial\tau^*_{Z\theta}}{\partial Z}\right], \tag{25}$$

$$\rho^*\left(V_R\frac{\partial V_Z}{\partial R}+V_Z\frac{\partial V_Z}{\partial Z}\right) = -\frac{\partial P^*}{\partial Z}+\left[\frac{1}{R}\frac{\partial}{\partial R}(R\tau^*_{RZ})+\frac{\partial\tau^*_{ZZ}}{\partial Z}\right], \tag{26}$$

$$\tau^* = \frac{1}{Re}\begin{bmatrix} 2\left(\frac{\partial V_R}{\partial R}-\frac{1}{3}\operatorname{div}^* V\right) & \left(\frac{\partial V_\theta}{\partial R}-\frac{V_\theta}{R}\right) & \left(\frac{\partial V_R}{\partial Z}+\frac{\partial V_Z}{\partial R}\right) \\ \left(\frac{\partial V_\theta}{\partial R}-\frac{V_\theta}{R}\right) & 2\left(\frac{V_R}{R}-\frac{1}{3}\operatorname{div}^* V\right) & \frac{\partial V_\theta}{\partial Z} \\ \left(\frac{\partial V_R}{\partial Z}+\frac{\partial V_Z}{\partial R}\right) & \frac{\partial V_\theta}{\partial Z} & 2\left(\frac{\partial V_Z}{\partial Z}-\frac{1}{3}\operatorname{div} V\right) \end{bmatrix}, \tag{27}$$

$$\rho^*\left(V_R\frac{\partial\theta}{\partial R}+V_Z\frac{\partial\theta}{\partial Z}\right) = \frac{1}{RePr}\left[\frac{1}{R}\frac{\partial}{\partial R}\left(R\frac{\partial\theta}{\partial R}\right)+\frac{\partial}{\partial Z}\left(\frac{\partial\theta}{\partial Z}\right)\right] + 0\beta^*\left(V_R\frac{\partial P^*}{\partial R}+V_Z\frac{\partial P^*}{\partial Z}\right)+E\nabla^* V:\tau^*, \tag{28}$$

$$\frac{P^*}{\rho^*} = R^*\theta, \tag{29}$$

$$V_R = 0 \quad \text{for} \quad Z=0, \quad 0<R<\frac{1}{2}, \tag{30}$$

$$Z=L^*, \quad 0<R<\frac{1}{2},$$

$$0<Z<L^*, \quad R=0,$$

$$0<Z<L^*, \quad R=\frac{1}{2},$$

$$V_Z = 0 \quad \text{for} \quad Z=0, \quad \frac{D_c}{2}<R<\frac{1}{2}, \tag{31}$$

$$Z=L^*, \quad 0<R<\frac{D_h}{2},$$

$$0<Z<L^*, \quad R=\frac{1}{2},$$

$$\frac{\partial V_Z}{\partial R}=0 \quad \text{for} \quad 0<Z<L^*, \quad R=0, \tag{32}$$

$$V_\theta = 0 \quad \text{for} \quad Z=0, \quad \frac{D_c}{2}<R<\frac{1}{2}, \tag{33}$$

$$Z=L^*, \quad 0<R<\frac{D_h}{2},$$

$$0<Z<L^*, \quad R=0,$$

$$\Delta<Z<L^*, \quad R=\frac{1}{2},$$

$$V_\theta = 1 \quad \text{for} \quad 0<Z<\Delta, \quad R=\frac{1}{2}, \tag{34}$$

$$P^* = P^*_0 \quad \text{for} \quad 0<Z<\Delta, \quad R=\frac{1}{2}, \tag{35}$$

$$P^* = P^*_\infty \quad \text{for} \quad Z=0, \quad 0<R<\frac{D_c}{2}, \tag{36}$$

$$Z=L^*, \quad \frac{D_h}{2}<R<\frac{1}{2},$$

$$\theta = 1 \quad \text{for} \quad 0<Z<\Delta, \quad R=\frac{1}{2}, \tag{37}$$

$$\frac{\partial\theta}{\partial R}=0 \quad \text{for} \quad \Delta<Z<L^*, \quad R=\frac{1}{2}, \tag{38}$$

$$0<Z<L^*, \quad R=0,$$

$$\frac{\partial\theta}{\partial Z}=0 \quad \text{for} \quad Z=0, \quad \frac{D_c}{2}<R<\frac{1}{2}, \tag{39}$$

$$Z=L^*, \quad 0<R<\frac{D_h}{2},$$

$$y+x=1, \tag{40}$$

$$y=\frac{2}{\Delta}\int_0^{D_c/2}\rho^*|V_Z|R\,dR, \tag{41}$$

$$x=\frac{2}{\Delta}\int_{D_h/2}^{1/2}\rho^* V_Z R\,dR, \tag{42}$$

$$y\left(\frac{\theta_c}{E}+\frac{V_{Zc}^2+V_{\theta c}^2}{2}\right)+(1-y)\left(\frac{\theta_h}{E}+\frac{V_{Zh}^2+V_{\theta h}^2}{2}\right) = \frac{1}{E}+\frac{1}{2}. \tag{43}$$

From the dimensionless system of equations, equations

(23)–(43), the functional dependence of $V_R$, $V_\theta$, $V_Z$, $P^*$, $\theta$, and $\rho^*$ can be represented by

$$\Phi_i = f_i(R, Z, D_c, D_h, \Delta, L^*, Re, Pr, E, R^*, \beta^*, P_0^*, P_\infty^*, y), \quad (44)$$

where $\Phi_i$ represents any one of the above-mentioned six dependent variables.

In this paper, we are especially interested in the temperature of the cold gas stream at its exit position $R = 0$ and $Z = 0$. To compare it later with experimental results, we are interested in the temperature difference $1-\theta_c = (T_0 - T_c)/T_0$ instead of $\theta_c = T_c/T_0$. Under these considerations equation (44) for the temperature of the cold gas stream at its exit position $R = 0$ and $Z = 0$ becomes

$$1-\theta_c = f(0, 0, D_c, D_h, \Delta, L^*, Re, Pr, E, R^*, \beta^*, P_0^*, P_\infty^*, y). \quad (45)$$

For geometrically similar vortex tubes the geometrical parameters $D_c$, $D_h$, $\Delta$, and $L^*$ are constant.

For such a case, equation (45) can be written as

$$1-\theta_c = f(Re, Pr, E, R^*, \beta^*, P_0^*, P_\infty^*, y). \quad (46)$$

As a first approximation, equation (46) can be presented, for a small operating range, by the following equation

$$1-\theta_c = f_1(Re) f_2(Pr) f_3(E) f_4(R^*) f_5(\beta^*) \times f_6(P_0^*) f_7(P_\infty^*) f_8(y). \quad (47)$$

Experiments indicate that $\theta_c$ has a minimum value, or $(1-\theta_c)$ has a maximum value, when $y$ varies from 0 to 1 and the other parameters are kept constant. The maximum value of $(1-\theta_c)$ can be determined by

$$(1-\theta_c)_{max} = f_1(Re) f_2(Pr) f_3(E) f_4(R^*) \times f_5(\beta^*) f_6(P_0^*) f_7(P_\infty^*) f_8(y_{max}). \quad (48)$$

Dividing equation (47) by equation (48), we obtain

$$\frac{1-\theta_c}{(1-\theta_c)_{max}} = \frac{f_8(y)}{f_8(y_{max})} = g(y). \quad (49)$$

Substituting the definition equation of $\theta_c$

$$\theta_c = \frac{T_c}{T_0},$$

into equation (49) and letting

$$\Delta T_c = T_0 - T_c$$

and

$$(\Delta T_c)_{max} = (T_0 - T_c)_{max},$$

we obtain from equation (49)

$$\frac{\Delta T_c}{(\Delta T_c)_{max}} = g(y). \quad (50)$$

Equation (50) indicates that the ratio of $\Delta T_c$ to $(\Delta T_c)_{max}$ is independent of the operating condition and the working medium in a vortex tube. Therefore, equation (50) is designated as the similarity relation for energy separation in a vortex tube.

## 4. EXPERIMENTAL VERIFICATION OF THE SIMILARITY RELATION

To verify the similarity relation obtained in the previous section, experiments were conducted. The

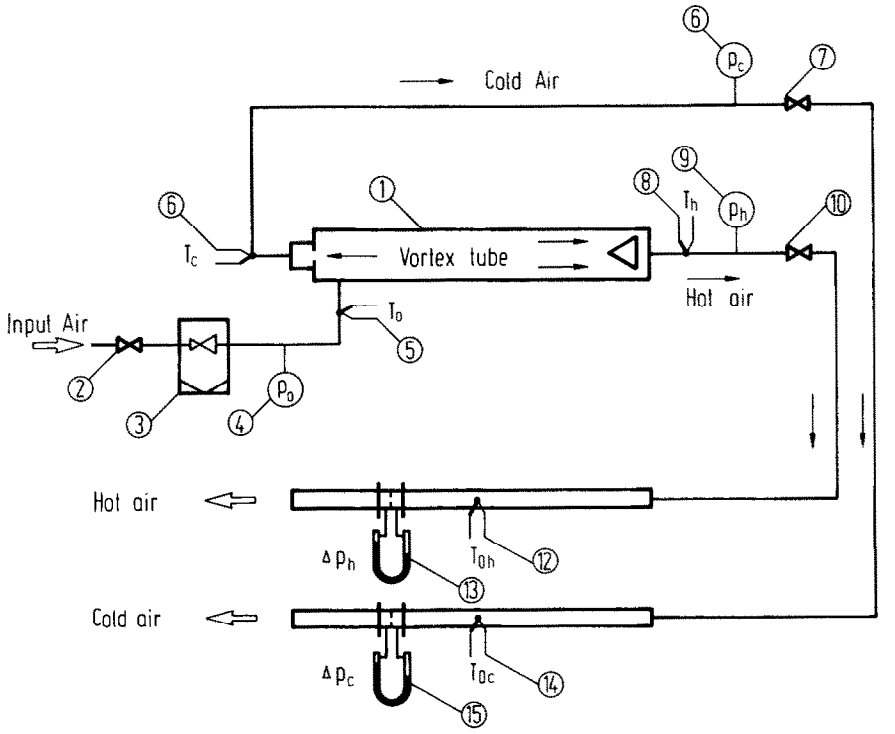


FIG. 2. Schematic diagram of the experimental apparatus.

experimental apparatus is shown schematically in Fig. 2. A compressed gas passing through the inlet valve (2) and the filter nozzle (3), is led tangentially into the vortex tube (1). The gas is expanded in the vortex tube and divided into a cold and a hot stream. The cold gas leaves the central orifice near the entrance nozzle, while the hot gas discharges at the periphery at the far end of the tube. The flow rate of the hot gas can be controlled by the control valve (10). The mass flow rates of the hot and cold gas are determined by measuring the pressure drops across the standard orifice devices (13) and (15) by using two Betz manometers, and the temperatures by using the thermocouples (12) and (14). The temperatures of the inlet gas, the cold and hot gas leaving the vortex tube, are measured by the thermocouples (5), (6), and (8), respectively. The pressure of the inlet gas is measured by the manometer (4). All temperatures measured by the thermocouples are recorded by a temperature recorder. The geometrical configuration of the experimental vortex tube is similar to one of the tubes used by Hilsch [2]. It was constructed with respect to a low cold gas temperature. The geometrical data of the vortex tube are as follows:

inner diameter $D = 17.6$ mm

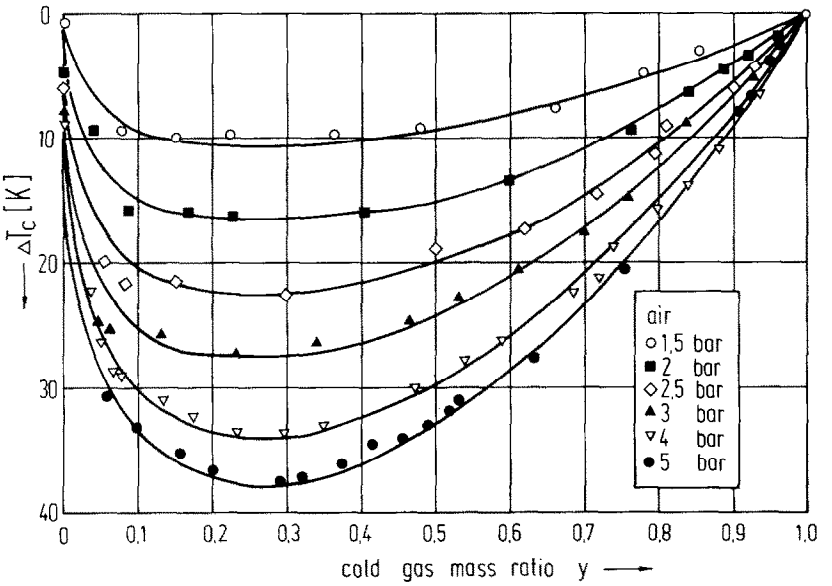


FIG. 3(a). Temperature difference, $\Delta T_c$, as function of the cold air mass ratio, $y$, with the pressure of the inlet air, $p_0$, as a parameter.

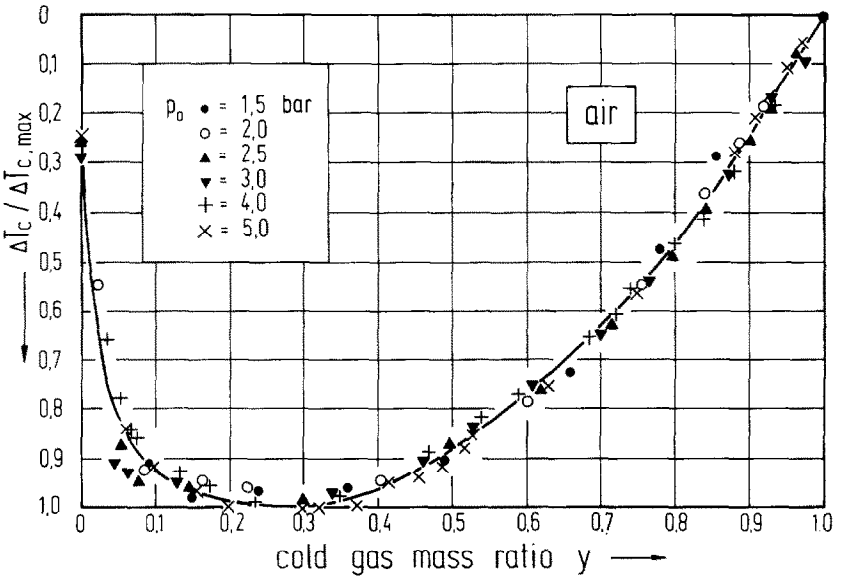


FIG. 3(b). Similarity relation compared with experimental data from Fig. 3(a).

| | |
|---|---|
| length | $L = 20D = 352$ mm |
| diameter of the inlet air nozzle | $\delta = 4.1$ mm |
| diameter of the cold exit air orifice | $d_c = 6.5$ mm. |

Three gases were used for the experiments: air, oxygen and helium. During the test, the gas inlet pressure $p_0$, and the cold gas mass ratio $y$ defined by:

$$y = \frac{\dot{m}_c}{\dot{m}_0} = \frac{\text{mass flow rate of the cold gas}}{\text{total gas mass flow rate}},$$

were varied systematically.

Figures 3(a), 4(a), and 5(a) show the experimental temperature differences between the inlet gas and the cold exit gas $\Delta T_c = T_0 - T_c$, as functions of the cold gas mass ratio $y$, with the gas inlet pressure $p_0$, as a parameter for air, oxygen, and helium as a working medium, respectively. From these figures, it is shown that for the case $y = 0$, without outflow of the cold gas, the temperature measured at the centre of the central orifice, which is used for the exit of the cold gas, is lower than the temperature of the inlet air, due to the effect of the energy separation. The energy separation process in the vortex tube is mainly determined by the inlet angular momentum of the working medium. An

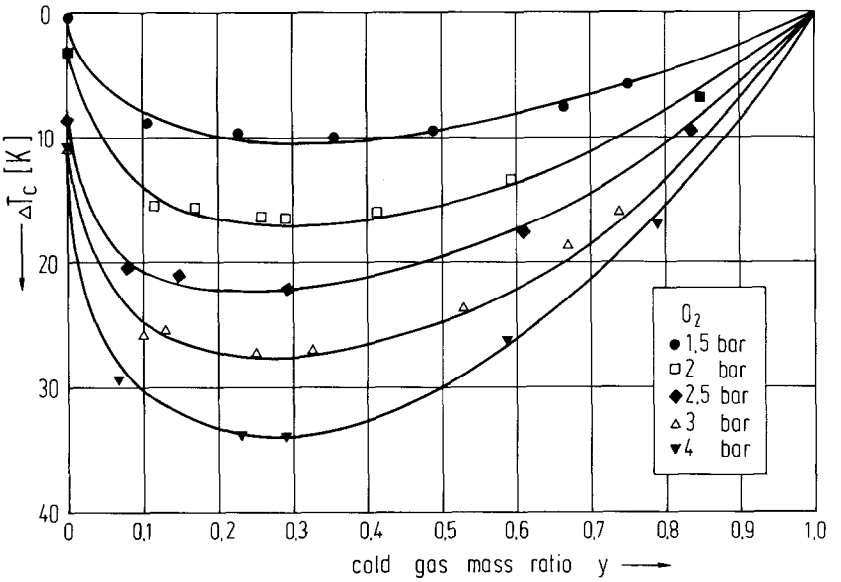


FIG. 4(a). Temperature difference, $\Delta T_c$, as function of the cold oxygen mass ratio, $y$, with the pressure of the inlet oxygen, $p_0$, as a parameter.

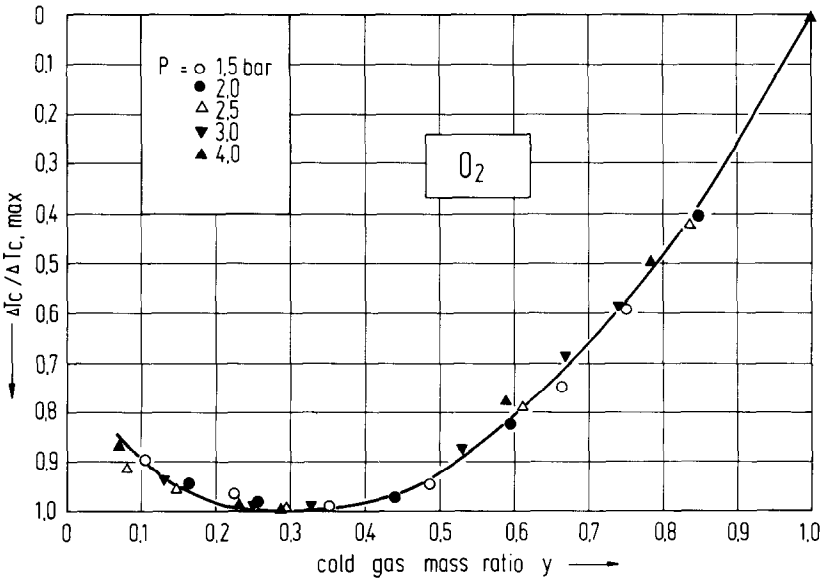


FIG. 4(b). Similarity relation compared with experimental data from Fig. 4(a).

increase in the gas inlet pressure $p_0$ causes an increase in the inlet angular momentum. Therefore, it is expected that, the higher the value of the gas inlet pressure $p_0$, the higher is the value of the cold gas temperature difference $T_c$ as shown in Figs. 3(a), 4(a), and 5(a).

In comparison to the experimental data plotted in Fig. 3(a) with those plotted in Fig. 4(a), it can be seen that there is practically no difference for the distributions of the cold gas temperature difference $\Delta T_c$ when air or oxygen is used as a working medium. On the other hand, the results obtained with helium [Fig. 5(a)] demonstrate that the energy separation in the vortex tube is much more effective than that with air or oxygen. This is due to the fact that the molecular weight of helium is much smaller than that of air or oxygen. In order to verify the similarity relation, equation (50), values of the ratio of $\Delta T_c/(\Delta T_c)_{max}$ were calculated from the experimental data. They are shown in Figs. 3(b), 4(b), and 5(b) for each substance and are plotted together in Fig. 6. They are represented by a single curve. Figure 7 shows the similarity relation $\Delta T_c/(\Delta T_c)_{max}$ as a function of $y$, obtained from the experimental results of Elser and Hoch [3] with five different gases and six gas inlet pressures for a fixed geometry. These experimental results can be represented by a single curve, too. The geometrical parameters of the vortex tube used in ref. [3] are $D = 4$ mm, $L = 200$ mm, $\delta = 1$ mm and $d_c = 2$ mm.

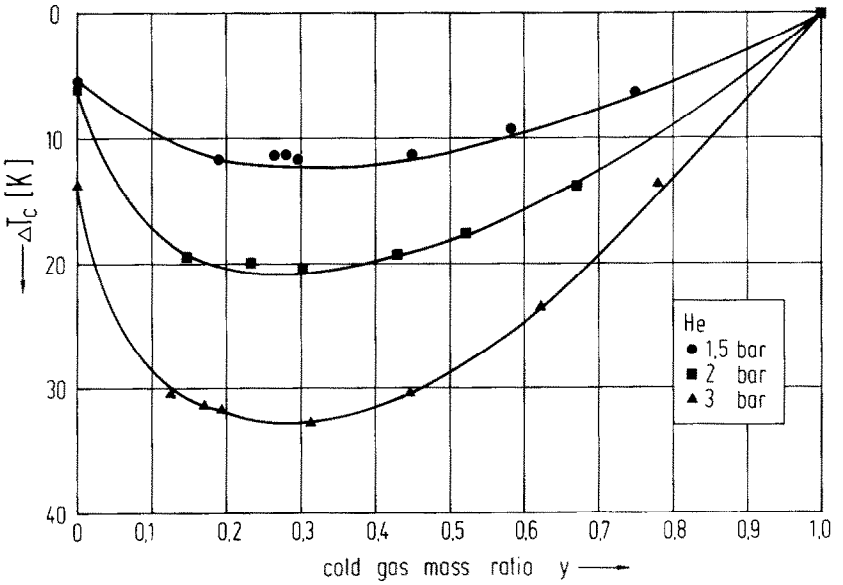


FIG. 5(a). Temperature difference, $\Delta T_c$, as function of the cold helium mass ratio, $y$, with the pressure of the inlet helium, $p_0$, as a parameter.

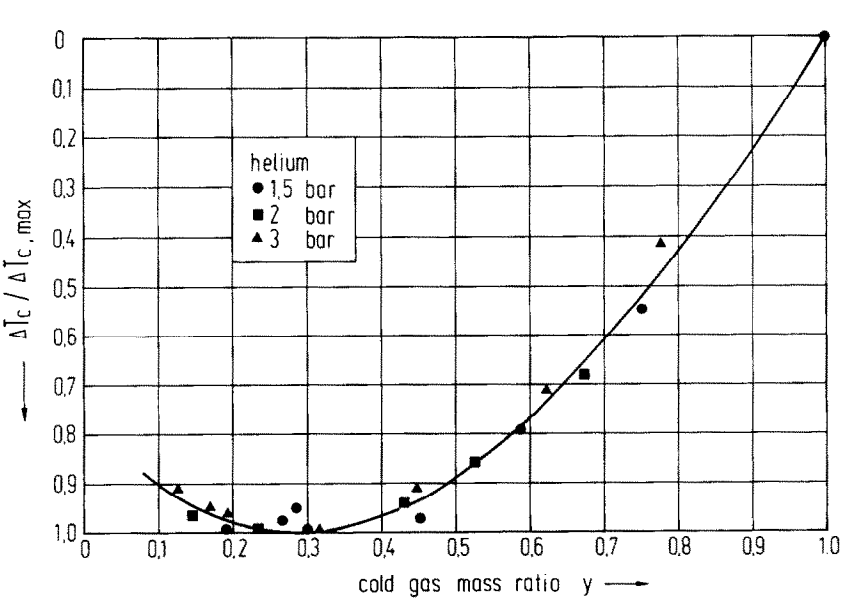


FIG. 5(b). Similarity relation compared with experimental data from Fig. 5(a).

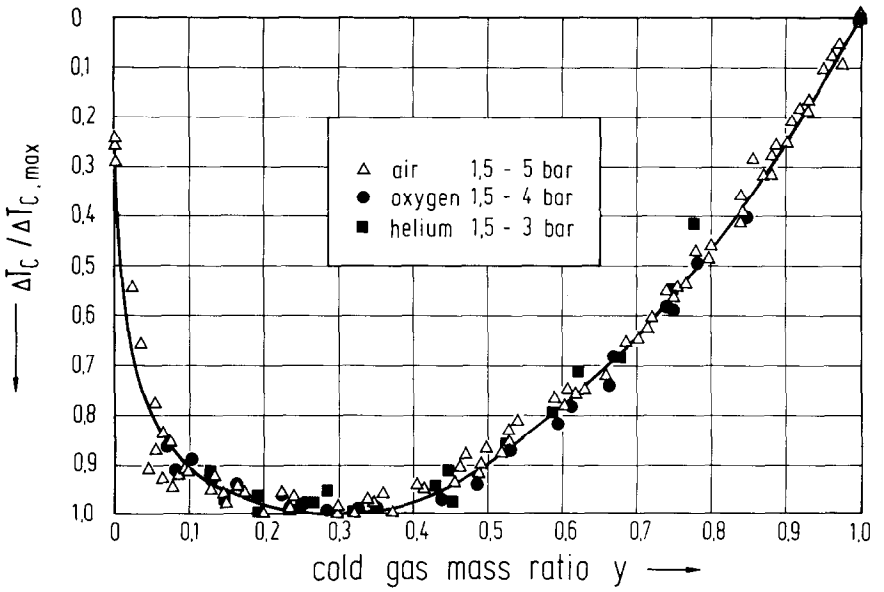


FIG. 6. Similarity relation compared with experimental data for air, oxygen and helium from Figs. 3(a), 4(a), and 5(a).

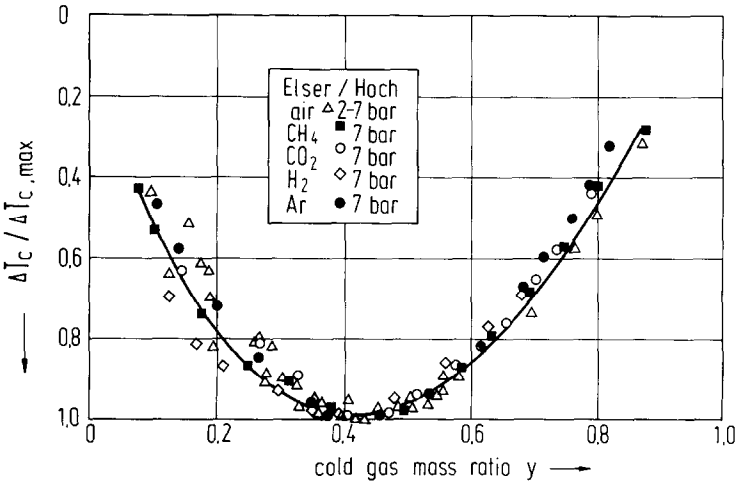


FIG. 7. Similarity relation compared with the experimental data of Elser and Hoch [3].

Figures 6 and 7 confirm that the ratio of $\Delta T_c/(\Delta T_c)_{max}$ is indeed independent of the operating conditions and the working medium in a vortex tube.

## 5. CONCLUSIONS

The system of equations (1)–(21) represents a general mathematical formulation of the energy separation process taking place in a vortex tube. From these equations, a similarity relation, the ratio of the actual temperature drop of the cold gas to the maximum temperature drop, $\Delta T_c/(\Delta T_c)_{max}$, can be represented as a function of the cold gas mass ratio. This similarity relation is independent from the operating conditions and the working substances in vortex tubes that are geometrically similar. Experimental data confirm the similarity relation.

*Acknowledgements*—The investigation was conducted at the Institut für Technische Thermodynamik und Thermische Verfahrenstechnik, Universität Stuttgart, Federal Republic of Germany, where S. Lin and F. Huang were visiting professors. S. Lin would like to express his gratitude to Deutsche Akademische Austauschdienst for financial support to participate in the research project.

## REFERENCES

1. G. Ranque, Expériences sur la détente giratoire avec productions simultanées d'un échappement d'air chaud et d'un échappement d'air froid, *J. Phys. Radium* **4**(7), 112–114 (1933).
2. R. Hilsch, Die Expansion von Gasen im Zentrifugalfeld als Kälteprozeß, *Z. Naturf.* **1**, 208–214 (1946).
3. K. Elser and M. Hoch, Das Verhalten verschiedener Gase und die Trennung von Gasgemischen in einem Wirbelrohr, *Z. Naturf.* **6a**, 25–31 (1951).

4. V. S. Martynovskii and V. P. Alekseev, Investigation of the vortex thermal separation effect for gases and vapors, *Soviet Phys.* 2233–2243 (1957).
5. H. Takahama, Studies on vortex tubes, *Bull. J.S.M.E.* **8**(31), 433–440 (1965).
6. J. P. Hartnett and E. R. G. Eckert, Experimental study of the velocity and temperature distribution in a high-velocity vortex-tube flow, *Trans. Am. Soc. Mech. Engrs*, Series C, *J. Heat Transfer* **79**, 751–758 (1976).
7. G. N. Bobrovnikov, A. A. Polyakov and N. J. Ilina, An investigation of a vortex tube working with humid air, *Kholod. Tekh.* **11**, 25–27 (1976) in Russian.
8. C. D. Fulton, Ranques tube, *Refrigng Engng* **5**, 473–479 (1950).
9. F. Schultz-Grunow, Turbulenter Wärmedurchgang im Zentrifugalfeld, *Forsch. Ing Wes.* **17**(3), 65–76 (1951).
10. J. Erdélyi, Wirkung des Zentrifugalfeldes auf den Wärmezustand der Gase, Erklärung der Ranque-Erscheinung, *Forsch. Geb. IngWes.* **28**(6), 181–186 (1962).
11. V. P. Alekseev and A. F. Azaroff, Development, investigation and application of non-adiabatic vortex tubes, Int. Cong. Refrig. (1978).
12. R. G. Deissler and M. Perlmutter, Analysis of the flow and energy separation in a vortex tube, *Int. J. Heat Mass Transfer* **1**, 173–191 (1960).
13. Yu. D. Raiskii and A. D. Sedykh, Using vortex tubes to cool natural gas, *Gazov. Prom.* **8**, 40–42 (1979) in Russian.
14. C. U. Linderstrøm-Lang, Gas separation in the Ranque–Hilsch vortex tube, *Int. J. Heat Mass Transfer* **7**, 1195–1206 (1964).
15. J. Marshall, Effect of operating conditions, physical size and fluid characteristics on the gas separation performance of the Linderstrøm-Lang vortex tube, *Int. J. Heat Mass Transfer* **20**, 227–231 (1977).
16. G. P. Igonin, O. Yu. Kozmin, N. A. Kostyannikov and M. P. Potapov, Evaluating the efficiency of the separation of gas mixtures in a vortex tube of pressures below the atmospheric, *Sov. Chem. Ind. Austin* **14**(5), 625–628 (1982).
17. K. Stephan, S. Lin, M. Durst, F. Huang and D. Seher, An investigation of energy separation in a vortex tube, *Int. J. Heat Mass Transfer* **26**, 341–348 (1983).
18. S. Whitaker, *Fundamental Principles of Heat Transfer*, Tables 5.1-1, 5.2-1 and 5.5-1. Pergamon Press, Oxford (1977).
19. E. Truckenbrodt, *Strömungsmechanik*, Tabelle 3.5. Springer, Berlin (1968).

## UNE RELATION DE SIMILITUDE POUR LA SEPARATION D'ENERGIE DANS UN TUBE A TOURBILLON

**Résumé**—On présente une formulation générale mathématique de la séparation d'energie qui s'opère dans un tube à tourbillon. A partir des équations fondamentales, on établit une relation en similitude de la variation de la température de sortie du gaz froid avec le rapport du débit masse de ce gaz, pour des tubes en similitude géométriques et on la compare à des résultats expérimentaux. Les expériences faites avec l'air, l'helium et l'oxygène confirment les considérations théoriques et elles correspondent bien avec la relation proposée.

## EINE ÄHNLICHKEITSBEZIEHUNG ZUR BESCHREIBUNG DER ENERGIEÜBERTRAGUNG IM WIRBELROHR

**Zusammenfassung**—Es wird eine allgemeine mathematische Beschreibung des Vorgangs der Energieübertragung, wie sie im Wirbelrohr stattfindet, vorgestellt. Ausgehend von den Bilanzgleichungen wird eine Ähnlichkeitsbeziehung hergeleitet. Mit dieser Gleichung kann für geometrisch ähnliche Wirbelrohre die erreichbare Abkühlung des Gases allein aus dem Kaltgasanteil berechnet werden. Eigene Versuche mit Luft, Helium und Sauerstoff sowie Vergleiche mit Literaturwerten bestätigen die theoretischen Überlegungen und stimmen mit der Ähnlichkeitsbeziehung sehr gut überein.

## СООТНОШЕНИЕ ПОДОБИЯ ДЛЯ РАСЧЕТА ВЫДЕЛЕНИЯ ЭНЕРГИИ В ВИХРЕВОЙ ТРУБКЕ

**Аннотация**—Представлена общая математическая формулировка процесса выделения энергии в вихревой трубке. На основе определяющих уравнений выведено соотношение подобия, описывающее изменение температуры холодного газа на выходе с изменением его массового числа для геометрически подобных вихревых трубок, и проведено сравнение с экспериментальными данными. Эксперименты, проведенные с воздухом, гелием и кислородом в качестве рабочих жидкостей, подтверждают результаты теоретических расчетов и хорошо описываются соотношением подобия.